A Journal of the Gesellschaft Deutscher Chemiker

Angewandte International Edition Chemie

GDCh

www.angewandte.org

Accepted Article

Title: Beyond the BET family: targeting CBP/p300 with 4-acyl pyrroles

Authors: Martin Hügle, Xavier Lucas, Dmytro Ostrovskyi, Pierre Regenass, Stefan Gerhardt, Oliver Einsle, Mirjam Hau, Manfred Jung, Bernhard Breit, Stefan Günther, and Daniel Wohlwend

To be cited as: *Angew. Chem. Int. Ed.* 10.1002/anie.201705516
Angew. Chem. 10.1002/ange.201705516

Link to VoR: http://dx.doi.org/10.1002/anie.201705516
http://dx.doi.org/10.1002/ange.201705516

WILEY-VCH

10.1002/anie.201705516

WILEY-VCH

COMMUNICATION

Beyond the BET family: targeting CBP/p300 with 4-acyl pyrroles

Martin Hügle, Xavier Lucas, Dmytro Ostrovskyi, Pierre Regenass, Stefan Gerhardt, Oliver Einsle, Mirjam Hau, Manfred Jung, Bernhard Breit, Stefan Günther and Daniel Wohlwend*

Abstract: BET bromodomain inhibitors are widely used both as chemical tools to study the biological role of their targets in living organisms, and as candidates for drug development against several cancer variants and human disorders. However, non-BET bromodomains such as those in p300 and CBP are less studied. Here, we introduce **XDM-CBP**, a highly potent and selective inhibitor for the bromodomains of CBP and p300 derived from a pan-selective BET BRD-binding fragment. In addition to X-ray crystal structure analysis and thermodynamic profiling, we used **XDM-CBP** in *in vitro* cell screenings of several cancer cell lines to study its inhibitory potential on cancer cell proliferation. Our results demonstrate that **XDM-CBP** is a potent and selective CBP/p300 inhibitor that acts on specific cancer cell lines, in particular malignant melanoma, breast cancer, and leukemia.

Small molecules inhibiting bromodomains (BDs) represent not only a novel approach to addressing specific malignancies driven or controlled by the epigenetic machinery, but also a valuable tool to study fundamental epigenetic mechanisms by means of chemical probes.[1] Most studies and drug discovery campaigns, however, focus on six members of the bromodomain and extra-terminal domain (BET) family. Especially, BRD4 is a proven drug target for fighting cancer, atherosclerosis, or diabetes.[2] Recently, great efforts have been made to identify inhibitors for BDs beyond the BET class.[2] In particular, the BD-containing cAMP response element-binding protein binding protein (CBP, also CREBBP) was shown to have a great potential for cancer treatment.[3] CBP and the close homologue E1A binding protein p300 (p300) co-activate transcription by bridging specific transcription factors with the basal transcription machinery.[4] They are also involved in chromatin relaxation through their histone acetyltransferase activity.[4] Similarly, they can directly acetylate transcription factors and thus modulate their activity. Finally, through their multiple domains, both proteins recruit a variety of proteins of the tumor immune response that moved them into the focus of oncology research.[5]

Within recent years four scaffolds could be identified that inhibit the BDs of CBP and p300 with nanomolar binding affinity (Supporting Table S1). In 2014, the first nanomolar CBP inhibitor scaffold was published, showing weak selectivity against BRD4(1) ($K_{D,CBP}$ = 390 nM, $K_{D,\ BRD4}$ = 1.4 µM, determined by isothermal titration calorimetry, ITC).[6] The chemical probe SGC-CBP30 belongs to a second class of CBP inhibitors (K_D = 21 nM, ITC) and is highly selective, although significant affinity was also observed to BRD4(1) (K_D = 850 nM, ITC).[7] This scaffold was optimized by Pfizer to give PF-CBP1 ($K_{D,CBP}$ = 190 nM, $K_{D,BRD4}$ > 20 µM, ITC, >100-fold selectivity). PF-CBP1 downregulates a number of inflammatory genes in macrophages as well as neuron specific genes, suggesting a therapeutic opportunity for CBP inhibitors in the treatment of neurological disorders.[8] I-CBP-112 belongs to the third CBP-inhibitor class ($K_{D,\ CBP}$ = 151 nM, $K_{D,BRD4}$ = 5.6 µM, ITC, 40-fold selectivity).[3] It notably reduces the leukemia-initiating potential of AML cells *in vitro* and *in vivo*. Most recently, Unzue and co-workers[9] presented a molecule with 33-fold selectivity ($K_{D,CBP}$ = 300 nM, ITC, $K_{D,BRD4(1)}$ = 9.9 µM, by competition assay) that acts on leukemia cell lines.

In this study we examined the inhibitory potential of fragments of our recently developed 4-acyl pyrrole based potent BET-inhibitor XD14[10] on CBP/p300. The core fragment XD46 still showed substantial affinity towards the BET family[11] but equally addressed CBP and p300 (Figure 1, Supporting Figure S1). Consequently, we set out to direct the selectivity of XD46 derivatives away from the BET family toward CBP/p300 using a combination of computational methods, chemical syntheses, X-ray crystallography, and ITC.

We initially grew XD46 inside the recognition site of p300 *in silico* and identified **XDM1** (Figure 1) with a *m*-chlorobenzyl attached to the amide anchor of XD46 (Syntheses for all compounds are given in the Supplementary Information). **XDM1**

[a] Dr. D. Wohlwend
Institut für Biochemie
Albert-Ludwigs-Universität Freiburg
Albertstr. 21, D-79104 Freiburg (Germany)
E-mail: wohlwend@bio.chemie.uni-freiburg.de
Prof. Dr. S. Günther
Institut für Pharmazeutische Wissenschaften and Freiburg Institute for Advanced Studies (FRIAS)
Albert-Ludwigs-Universität Freiburg
Hermann-Herder-Str. 9, D-79104 Freiburg (Germany)
E-mail: stefan.guenther@pharmazie.uni-freiburg.de
[b] M. Hügle,[+] Dr. S. Gerhardt
Institut für Biochemie
Albert-Ludwigs-Universität Freiburg
Albertstr. 21, D-79104 Freiburg (Germany)
Dr. X. Lucas[+]
School of Life Sciences, Division of Biological Chemistry and Drug Discovery
University of Dundee, James Black Centre
Dow Street, Dundee, DD1 5EH (United Kingdom)
Prof. Dr. O. Einsle
Institut für Biochemie, Freiburg Institute for Advanced Studies (FRIAS) and BIOSS Centre for Biological Signalling Studies
Albert-Ludwigs-Universität Freiburg
Albertstr. 21, D-79104 Freiburg (Germany)
Dr. D. Ostrovskyi,[+] Dr. P. Regenass
Institut für Organische Chemie
Albert-Ludwigs-Universität Freiburg
Albertstr. 21, D-79104 Freiburg (Germany)
Prof. Dr. B. Breit
Institut für Organische Chemie and Freiburg Institute for Advanced Studies (FRIAS)
Albert-Ludwigs-Universität Freiburg
Albertstr. 21, D-79104 Freiburg (Germany)
M. Hau, Prof. Dr. M. Jung
Institut für Pharmazeutische Wissenschaften
Albert-Ludwigs-Universität Freiburg
Albertstr. 25, D-79104 Freiburg (Germany)

[+] These authors contributed equally to this work

Supporting information for this article is given via a link at the end of the document

10.1002/anie.201705516

has moderate affinity to both targets, slightly favoring p300 over CBP (Supporting Figure S2).

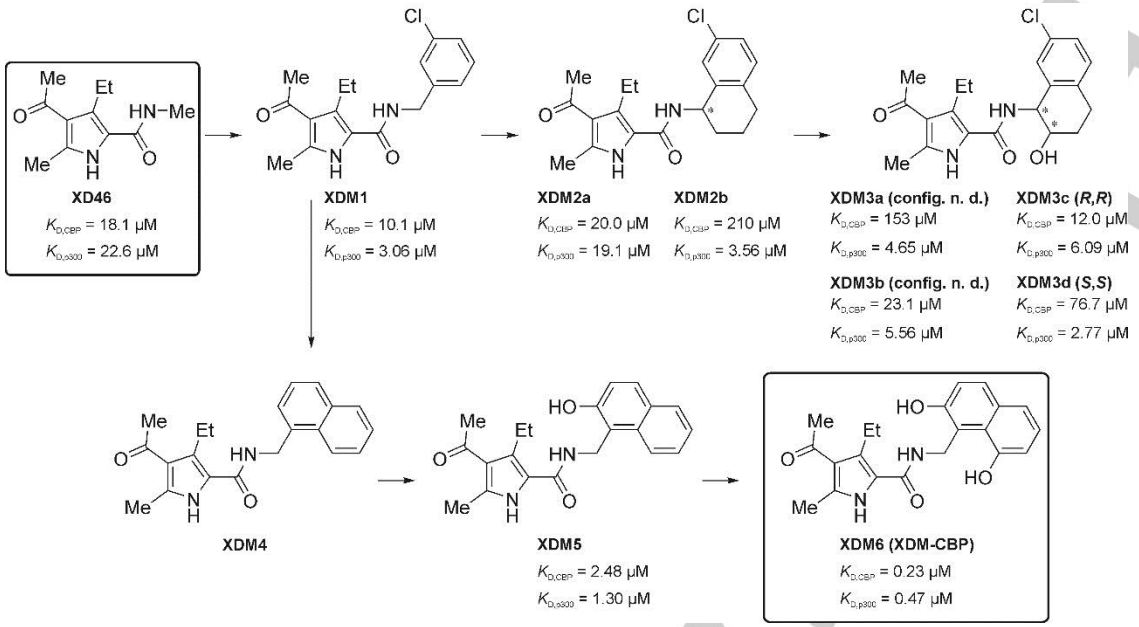

Figure 1. Chemical structures of compounds explored during the development of XDM-CBP based on fragment XD46. K_D values were determined by ITC.

The crystal structure of **XDM1** in complex with CBP (Figure 2A) confirmed that it binds to the recognition pocket of CBP with five well-conserved water molecules surrounding its 4-acyl pyrrole core.[12] In addition, the structure presents an induced-fit binding mode of Pro1110 and Arg1173.[6] As setting up this cavity depends on binding of a suitable ligand, we designate this motif the inducible RP cavity. In complex with p300, **XDM1** presents a similar yet more heterogeneous binding, exemplified by three slightly different binding modes (Supporting Figure S12). Analysis of the crystal structures of **XDM1** with both p300 and CBP using SiteMap (Schrödinger, LLC, New York, NY, USA) revealed a hydrophobic region within the ZA channel (Supporting Figure S13). To address it and at the same time reduce the flexibility of the chlorobenzyl moiety, we next introduced a 7-chloro-1,2,3,4-tetrahydronaphthalenyl moiety, thus fixing the *m*-chlorobenzyl system (**XDM2**, Figure 1). The two resulting enantiomers, **XDM2a** and **XDM2b**, were separated by means of chiral HPLC and characterized by ITC (Supporting Figures S3-4). **XDM2a** lost affinity and fell back to the level of the starting fragment XD46. **XDM2b** exhibited an apparent 59-fold selectivity toward p300 over CBP, primarily by losing affinity toward the latter (Figure 1). However, both molecules lacked an adequate solubility due to their increased hydrophobicity (c$\log P_{o/w}$ = 4.99), questioning the reliability of the affinity determination by ITC and undermining any attempts of co-crystallization with p300 or CBP. Accordingly, the absolute configuration of their stereocenters and more reliable affinities remain unresolved.

Consequently, we added a hydroxyl group at the C2 of the 7-chloro-1,2,3,4-tetrahydronaphthyl moiety to increase water solubility, yielding **XDM3** (Figure 1, c$\log P_{o/w}$ = 3.96). The second chiral center gives rise to four stereoisomers, the compounds **XDM3a**-**d** that were separated by means of chiral HPLC. ITC validation of these compounds showed good binding of p300 to all of them (Figure 1 and Supporting Figures S5-8). **XDM3b** and **XDM3c** are still recognized by CBP (Supporting Figures S6 and S7), while **XDM3a** and **XDM3d** failed to interact tightly with CBP (Supporting Figures S5 and S8). Their selectivity toward p300 resembles that of **XDM2b**, suggesting that the shared absolute configuration of the carbon atom C1 of **XDM3a** and **XDM3d** is identical to the one of **XDM2b**. X-ray crystal structures of **XDM3c** bound to CBP and **XDM3d** bound to p300 (Figure 2B, Supporting Figure S14) allowed for the determination of the absolute configurations as (*R*,*R*) and (*S*,*S*), respectively. Both structures conserve the interaction of the 4-acyl pyrrole moiety with the KAc binding site. However, in CBP, flipping of the amide linker of **XDM3c** induces two slightly different positions of the tetrahydronaphthyl moiety, whereas in complex with p300, the amide of **XDM3d** is fixed in one orientation that forces the tail to address the ZA channel we initially aimed at. Here, **XDM3d** replaces a surface-bound water molecule close to Asp1080 at the back of the ZA channel, allowing for an interaction of its π-system with the amide head group of Gln1077. However, Arg1137, which was hypothesized to form an inducible RP cavity with Pro1074, does not participate in binding. Rather Arg1137 appears to be constitutively locked in a remote position of the binding pocket by Tyr1141. Notably, the good discriminatory potential of **XDM3d** with respect to CBP and p300 (28-fold selectivity) does not fully apply to other bromodomains, in particular members of the BET family (Supporting Figure S9). Moreover, in the crystal structure we identified two additional binding modes of **XDM3d** to the surface of p300 that could not be further resolved by ITC (Supporting Figures S8 and S15).

10.1002/anie.201705516

COMMUNICATION

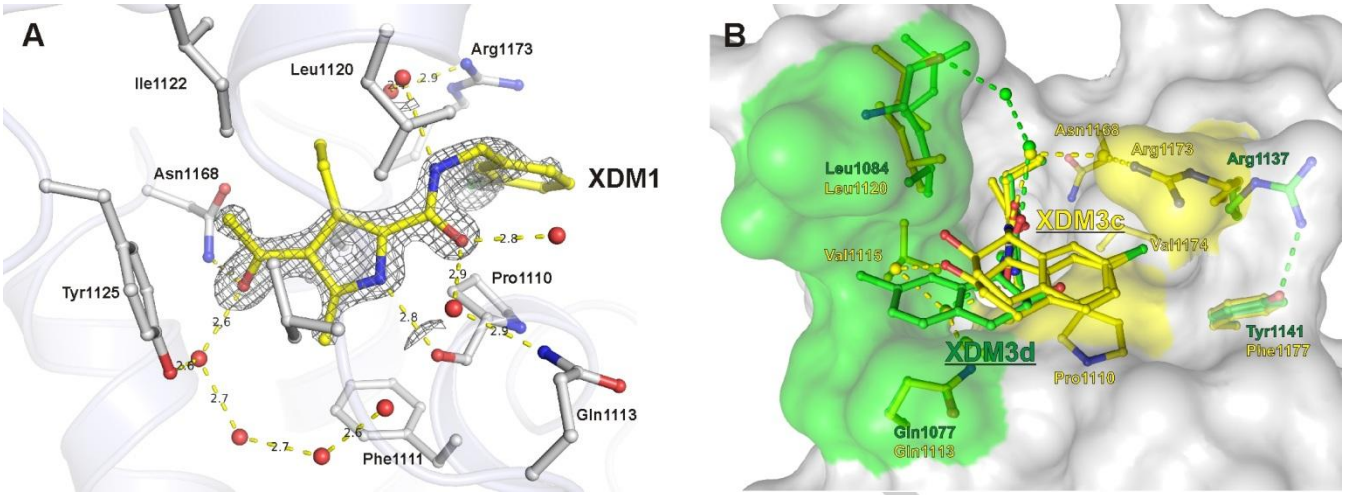

Figure 2. Crystal structures of **XDM1** and **XDM3c** in complex with CBP and of **XDM3d** bound to p300. (A) **XDM1** is recognized by Asn1168 in the KAc binding site of CBP and stabilized by hydrogen bonds and van der Waals contacts to the hydrophobic pocket core. The 2Fo-Fc omit map at 1.0 σ is shown for **XDM1**. (B) Superposition of the KAc binding sites of CBP bound to **XDM3c** and p300 bound to **XDM3d**. **XDM3c** (yellow sticks) occupies the inducible RP cavity of CBP (yellow sticks and surface, shown for CBP), while **XDM3d** (green sticks) binds to the ZA channel of p300 (green side chains and surface, shown for p300). Differing hydrogen bonds and bridging waters are colored accordingly.

In order to restrict inhibitor binding to the KAc binding site and to enhance specificity, we focused on improving the surface complementarity and supporting the π-stacking by introducing a (naphthalene-1-yl)methyl moiety to **XDM1**, yielding **XDM4** (Figure 1). The hydrophobicity of this tail resulted in a weak water solubility, preventing successful measurements by ITC. However, we obtained a high-resolution crystal structure of XDM4 in complex with CBP (Supporting Figure S16). The 4-acyl pyrrole head exploits the already well-described interactions with CBP. The amide linker is placed like previously shown for **XDM1**. As expected, the extended aromatic tail points towards Arg1173, thus occupying the inducible RP cavity of CBP.

To increase water solubility and further optimize target affinity by pursuing an intra-molecular hydrogen bond (IMHB), a hydroxyl group was introduced to the tail of **XDM4**, yielding **XDM5** (Figure 1). Although attempts to obtain a crystal structure of **XDM5** in complex with either CBP or p300 were not successful, the affinity to p300 and to CBP was overall substantially improved compared to **XDM3** (Figure 1, Supporting Figure S10).

We added a second hydroxyl group to **XDM5**, producing **XDM6** (Figure 1). This should allow for additional IMHBs to minimize the rotation of the tail. The co-crystal structures of **XDM6** with CBP and p300 reveal poses similar to previously described **XDM4** (Figure 3). The structures confirm the establishment of two IMHBs between the amide linker and the novel hydroxyl groups of **XDM6** that lock the conformation of the 2,8-dihydroxynaphthalen-1-yl)methyl moiety (Supporting Figures S16 and S17). This is supported by the low B-factors of this moiety (average B-factors of 17.8 Å^2 for CBP and 18.6 Å^2 for p300 with overall B-factors of 18.5 Å^2 and 20.1 Å^2, respectively, Supporting Table S2). A structural comparison with other CBP-inhibitor complexes reveals that **XDM6** is the only inhibitor that is intrinsically fixed in a conformation that apparently induces a rigid rotamer fit of Arg1173 (CBP) and Arg1137 (p300, Figure 3B, Supporting Figure S20A). ITC analysis highlighted the benefits of the additional IMHB by disclosing significantly improved entropy contributions to binding (Supporting Figure S11A) that resulted in nanomolar affinities to both proteins and a ligand efficiency (LE) for CBP of -0.33 kcal/mol. To our knowledge, this is the highest LE for a nanomolar CBP inhibitor reported to date. In addition, **XDM6** features a good lipophilic LE (LLE) of 3.22 (c$\log P_{o/w}$ = 3.40), outperformed only by compound 19[9] of Unzue and co-workers (LLE 3.56, Supporting Table S1). In addition, competition assays by ITC with the established CBP inhibitor I-CBP-112[3] show that **XDM6** and I-CBP-112 address the same site in the BD of CBP and that their binding is mutually exclusive (Supporting Figure S11B-C), demonstrating that the mode of action of **XDM6** on the BD of CBP is identical to I-CBP-112.

We next tested the specificity of **XDM6** in a bromoKdELECT screen (DiscoveRx) against 40 BDs (Figure 4A, Supporting Figure S18). In comparison with the BET-inhibitor XD14,[10] the specificity of **XDM6** is redirected from the BET family towards CBP/p300, having only little residual affinity to BRD9 (K_D = 2.9 μM), BRD7 (K_D = 4.5 μM), BRD2(1), BRPF1 and BRPF3 (all close to 10 μM), while all other bromodomains, including BRD4(1), are not recognized under the test conditions (K_D > 40 μM). The avoidance of BET BDs can be assigned to the IMHBs in **XDM6** that makes a conformational change to adapt to the KAc binding site of BRD4(1) energetically disfavored (Supporting Figures S17 and S20B). Hence, we name this compound **XDM-CBP**.

Finally, we assessed the antiproliferative activity of **XDM-CBP** in the NCI60[13] panel provided by the National Cancer Institute (NCI, NIH, Rockville, MD, US). While XD14 mainly targeted leukemia cell lines (Supporting Figures S19 and S27), **XDM-CBP** is potent on numerous cancer variants (Figure 4B, Supporting Figure S26), including leukemia (mean growth inhibition at 10 μM for 48h (GI) of 77%), breast cancer (GI = 74 %), and melanoma (GI = 73 %). Its potency peaks for individual cell lines of melanoma (SK-MEL-5), breast cancer (T-47D), and non-small cell lung cancer (NCI-H522).

10.1002/anie.201705516
WILEY-VCH

COMMUNICATION

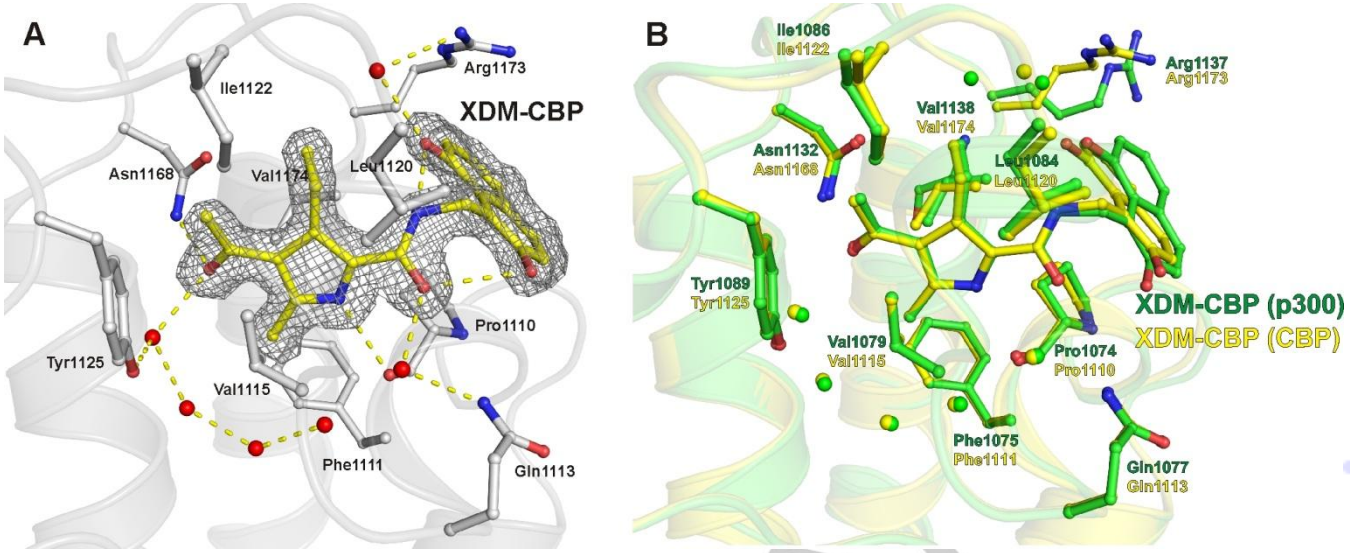

Figure 3. Binding of **XDM-CBP** to CBP and p300. (A) Recognition of **XDM-CBP** by CBP is driven by binding of the 4-acyl pyrrole moiety to the KAc binding site and by the interaction of the naphthalenyl moiety with the inducible RP cavity. (B) Superposition of the KAc binding sites of p300 (green) and CBP (yellow) in complex with **XDM-CBP**. The binding mode is largely conserved with only minor differences in the naphthalenyl position.

A detailed analysis of the antiproliferative effect on HL-60 and MCF-7 cells (Supporting Figure S30) yielded GI_{50} values of 1.3 µM (HL-60) and 4.2 µM (MCF-7). Here, **XDM-CBP** proves to be more efficient than I-CBP-112 in both cell lines, which might by due to a better LLE of **XDM-CBP** (LLE of 3.22) as compared to I-CBP-112 (LLE of 2.68, Supporting Table S1). Interestingly, MCF-7 cells remain largely unaffected by (+)-JQ1 treatment, a well characterized BET inhibitor,[14] supporting the discriminatory potential of **XDM-CBP** against BET BDs.

Our results demonstrate that **XDM-CBP**, the final product of the optimization, is an excellent CBP/p300 inhibitor that combines outstanding ligand efficiency with high selectivity for CBP/p300 over all other BD families, including the BET family. Most importantly, **XDM-CBP** has an antiproliferative effect on numerous cancer cell lines. This renders **XDM-CBP** a serious candidate for further optimization towards initial clinical studies and it supports the high potential of 4-acyl pyrrole derivatives for the development of inhibitors and therapeutic agents beyond the BET BD family.

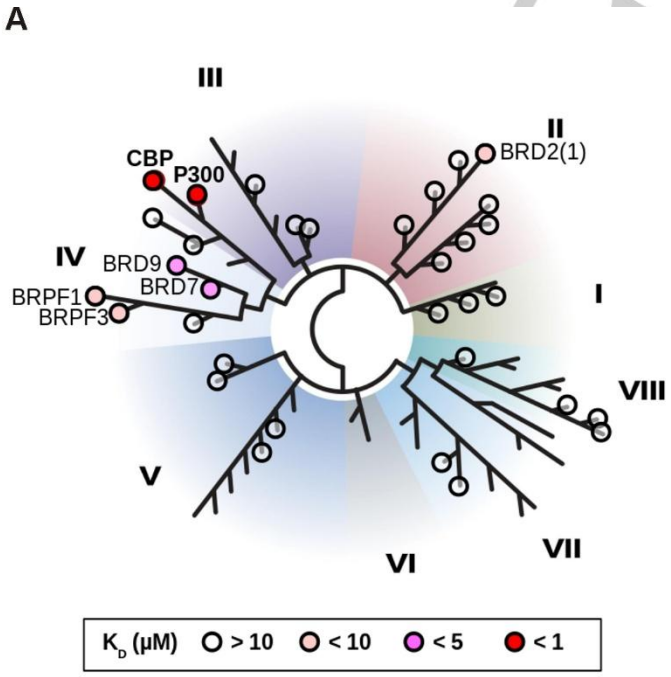

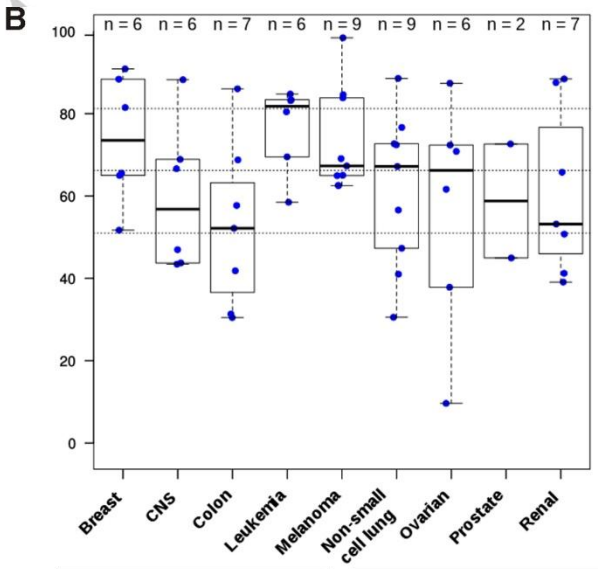

Most sensitive cell lines			
Cell line	Cancer variant	GI (%)	Z-score
SK-MEL-5	Melanoma	98.4	1.8
T-47D	Breast	90.9	1.4
NCI-H522	Non-Small Cell Lung	88.6	1.3
ACHN	Renal	88.4	1.3
MCF7	Breast	88.4	1.3

Most resistant cell lines			
Cell line	Cancer variant	GI (%)	Z-score
OVCAR-5	Ovarian	9.6	-2.9
COLO 205	Colon	30.5	-1.8
NCI-H322M	Non-Small Cell Lung	30.5	-1.8
SW-620	Colon	31.3	-1.7
SK-OV-3	Ovarian	37.8	-1.4

Figure 4. Specificity and antiproliferative activity of **XDM-CBP**. (A) Phylogenetic tree of the human BD family with selectivity profiles of **XDM-CBP**. Sphere colors indicate the binding affinity to specific BDs, as observed in the BROMO*scan* assay. (B) Antiproliferative activity of **XDM-CBP**. Top: Box plot of the sensitivity of cancer cells covered by the NCI60 panel. Bottom: Top 5 ranked cell lines regarding sensitivity and resistance.

Acknowledgements

This work was financially supported by the DFG (GU1225/3-1, X. L., and WO2012/1-1, M. H.). S. G., D. O., B. B., M. J., and O. E. received funding from the DFG (CRC 992 'Medical Epigenetics'). The authors thank the staff of the Swiss Light Source (SLS) beamlines X06SA and X06DA for excellent technical support.

Keywords: bromodomains • CBP • p300 • drug discovery • 4-acyl pyrroles

[1] T. Fujisawa, P. Filippakopoulos, *Nat. Rev. Mol. Cell Biol*. **2017**, *18*, 246-62.

[2] N. H. Theodoulou, N. C. Tomkinson, R. K. Prinja, P. G. Humphreys, *Curr. Opin. Chem. Biol.* **2016**, *33*, 58-66.

[3] S. Picaud, O. Fedorov, A. Thanasopoulou, K. Leonards, K. Jones, J. Meier, H. Olzscha, O. Monteiro, S. Martin, M. Philpott, A. Tumber, P. Filippakopoulos, C. Yapp, C. Wells, K. H. Che, A. Bannister, S. Robson, U. Kumar, N. Parr, K. Lee, D. Lugo, P. Jeffrey, S. Taylor, M. L. Vecellio, C. Bountra, P. E. Brennan, A. O'Mahony, S. Velichko, S. Müller, D. Hay, D. L. Daniels, M. Urh, N. B. La Thangue, T. Kouzarides, R. Prinjha, J. Schwaller, S. Knapp, *Cancer Res.* **2015**, *75*, 5106-19.

[4] N. Shiama, *Trends Cell Biol.* **1997**, *7*, 230-6.

[5] F. A. Romero, A. M. Taylor, T. D. Crawford, V. Tsui, A. Côté, S. Magnuson, *J. Med. Chem.* **2016**, *59*, 1271-98.

[6] T. P. Rooney, P. Filippakopoulos, O. Fedorov, S. Picaud, W. A. Cortopassi, D. A. Hay, S. Martin, A. Tumber, C. M. Rogers, M. Philpott, M. Wang, A. L. Thompson, T. D. Heightman, D. C. Pryde, A. Cook, R. S. Paton, S. Muller, S. Knapp, P. E. Brennan, S. J. Conway, *Angew. Chem. Int. Ed. Engl.* **2014**, *53*, 6126-30.

[7] D. A. Hay, O. Fedorov, S. Martin, D. C. Singleton, C. Tallant, C. Wells, S. Picaud, M. Philpott, O. P. Monteiro, C. M. Rogers, S. J. Conway, T. P. Rooney, A. Tumber, C. Yapp, P. Filippakopoulos, M. E. Bunnage, S. Muller, S. Knapp, C. J. Schofield, P. E. Brennan, *J. Am. Chem. Soc.* **2014**, *136*, 9308-19.

[8] E. L. Chekler, J. A. Pellegrino, T. A. Lanz, R. A. Denny, A. C. Flick, J. Coe, J. Langille, A. Basak, S. Liu, I. A. Stock, P. Sahasrabudhe, P. D. Bonin, K. Lee, M. T. Pletcher, L. H. Jones, *Chem. Biol.* **2015**, *22*, 1588-96.

[9] A. Unzue, M. Xu, J. Dong, L. Wiedmer, D. Spiliotopoulos, A. Caflisch, C. Nevado, *J. Med. Chem.* **2016**, *59*, 1350-6.

[10] X. Lucas, D. Wohlwend, M. Hügle, K. Schmidtkunz, S. Gerhardt, R. Schüle, M. Jung, O. Einsle, S. Günther, *Angew. Chem. Int. Ed. Engl.* **2013**, *52*, 14055-9.

[11] M. Hügle, X. Lucas, G. Weitzel, D. Ostrovskyi, B. Breit, S. Gerhardt, O. Einsle, S. Günther, D. Wohlwend, *J. Med. Chem.* **2016**, *59*, 1518-30.

[12] M. Xu, A. Unzue, J. Dong, D. Spiliotopoulos, C. Nevado, A. Caflisch, *J. Med. Chem.* **2016**, *59*, 1340-9.

[13] R. H. Shoemaker, *Nat. Rev. Cancer* **2006**, *6*, 813-23.

[14] P. Filippakopoulos, J. Qi, S. Picaud, Y. Shen, W. B. Smith, O. Fedorov, E. M. Morse, T. Keates, T. T. Hickman, I. Felletar, M. Philpott, S. Munro, M. R. McKeown, Y. Wang, A. L. Christie, N. West, M. J. Cameron, B. Schwartz, T. D. Heightman, N. La Thangue, C. A. French, O. Wiest, A. L. Kung, S. Knapp, J. E. Bradner, *Nature* **2010**, *468*, 1067-73.

10.1002/anie.201705516

WILEY-VCH

COMMUNICATION

XDM-CBP is a selective, potent and cell active CBP/p300 inhibitor

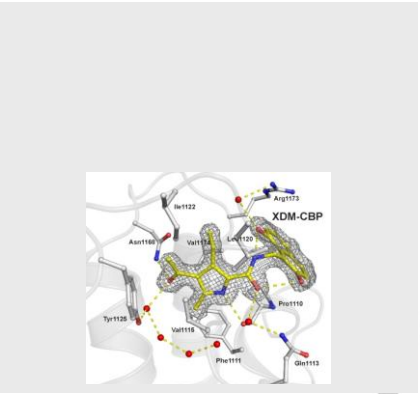

*Martin Hügle, Xavier Lucas, Dmytro Ostrovskyi, Pierre Regenass, Stefan Gerhardt, Oliver Einsle, Bernhard Breit, Stefan Günther and Daniel Wohlwend**

Page No. – Page No.
Beyond the BET family: targeting CBP/p300 with 4-acyl pyrroles